

Accepted Manuscript

Internal characterization of embankment dams using ground penetrating radar (GPR) and thermographic analysis: A case study of the Medau Zirimilis Dam (Sardinia, Italy)

Ó. Pueyo Anchuela, P. Frongia, F. Di Gregorio, A.M. Casas Sainz, A. Pocoví Juan



PII: S0013-7952(16)30608-1
DOI: doi:[10.1016/j.enggeo.2018.02.015](https://doi.org/10.1016/j.enggeo.2018.02.015)
Reference: ENGEO 4773

To appear in: *Engineering Geology*

Received date: 5 November 2016

Revised date: 21 February 2018

Accepted date: 21 February 2018

Please cite this article as: Ó. Pueyo Anchuela, P. Frongia, F. Di Gregorio, A.M. Casas Sainz, A. Pocoví Juan, Internal characterization of embankment dams using ground penetrating radar (GPR) and thermographic analysis: A case study of the Medau Zirimilis Dam (Sardinia, Italy). The address for the corresponding author was captured as affiliation for all authors. Please check if appropriate. *Enggeo*(2018), doi:[10.1016/j.enggeo.2018.02.015](https://doi.org/10.1016/j.enggeo.2018.02.015)

This is a PDF file of an unedited manuscript that has been accepted for publication. As a service to our customers we are providing this early version of the manuscript. The manuscript will undergo copyediting, typesetting, and review of the resulting proof before it is published in its final form. Please note that during the production process errors may be discovered which could affect the content, and all legal disclaimers that apply to the journal pertain.

Internal characterization of embankment dams using ground penetrating radar (GPR) and thermographic analysis: A case study of the Medau Zirimilis Dam (Sardinia, Italy).

Pueyo Anchuela, Ó.^{1,*} opueyo@gmail.com., Frongia, P.², Di Gregorio, F.², Casas Sainz, A.M.¹ acasas@unizar.es, Pocoví Juan, A.¹ apocovi@unizar.es

¹Grupo de Investigación Geotransfer. Instituto de Investigación en Ciencias Ambientales (IUCA). Universidad de Zaragoza. C/Pedro Cerbuna, nº12. CP. 50009. Zaragoza (Spain)

²Facoltà di Scienze. Università degli Studi di Cagliari. Via Università 40, 09124 Cagliari (Sardinia, Italy). paolofron@gmail.com; digregof@unica.it.

*Corresponding author at: Grupo de Investigación Geotransfer. Instituto de Investigación en Ciencias Ambientales (IUCA). Universidad de Zaragoza. C/Pedro Cerbuna, nº12, CP. 50009. Zaragoza (Spain). 0034 976762127.

Abstract

The stability of embankment dams without an impermeable core depends on the characteristics of the face slab that prevents internal erosion, piping and eventual collapse of the structure. Under a Mediterranean climate, the impermeable asphaltic face slab is subjected to high solar radiation and consequent temperature changes, which can generate the creation of cracks and joints. The Medau Zirimilis dam, located in the Casteddu River (Sardinia), is an embankment dam that has undergone seepage and continuous repairs in its asphalt face slab. These reparations have been conducted because of the occurrence of cracks and relative movement of different segments of the slab. To evaluate if seepage endangers the integrity of the dam, GPR was used, with different antennas (100, 250 and 500 MHz), along its crest and upstream and downstream faces, and the data were integrated with infrared thermographic images. Although geophysical data do not show structural changes affecting the main dam structure, deformation structures at shallow levels and in particular in the upstream face and along the crest of the dam have been identified. Such deformation affects the road atop the crest, the face slab and underlying levels, resulting in landslides that include material from several meters below the surface. The analysis permitted the identification of the origin of surficial cracks and their effects on the face slab. These sectors, independent of current

movement, define the most unstable areas against water level changes that can affect the dam integrity. GPR analysis at the embankments usually has the handicap of high clay content that precludes electromagnetic wave penetration; however, in this case, the obtained resolution and extent of penetration using the different antennas was sufficient, due to the absence of an inner waterproof unit, and permitted the evaluation of the inner structure of the dam and the application of GPR for construction quality surveillance, internal structural characterization and dam monitoring.

Keywords: embankment dam, structural damage, GPR, Sardinia, TIR

1. Introduction

Dam, levee and embankment stability depends upon the geological characteristics, construction design and materials used, together with their interaction with water and the hydraulic gradient on both sides of the structure. From a statistical point of view, the Icold Bulletin stated in 2013 that between 1800 and 1986, 80 embankment dams failed during their lifetime; 94% of failures were related to erosion and 6% to sliding or slope instability. Middlebrooks (1952), for the period 1850–1950 in the United States, found that dam failure was in 30% of the cases due to overtopping, whereas piping and upstream failure represented 25% and 5% of cases, respectively. Failures with variable mechanisms represented 15% of total dam failures, where slope protection damage is responsible for numerous dam incidents (Kollgaard and Chadwick, 1988). These data indicate that the construction characteristics and the changes occurring during dam development, especially as related to water level changes, hydraulic pressure and modifications, are closely related to dam failures. In this sense, monitoring, stability testing and continuous surveillance are needed to avoid undesirable or catastrophic consequences (Costa and Schuster, 1988; Zhang and Chen, 2006; Bolève et al., 2009; Loperte et al., 2016).

Different approaches have been employed for the evaluation of the stability of dams, the identification of their internal structure and potential changes that dams can undergo following construction. Both direct and indirect approaches have been employed in dam monitoring including the search for cavities, leakage zones and structural damage (e.g., Kocbay and Kilic,

2006; Sjö Dahl et al., 2008; Loperte et al., 2011; AalGamal et al., 2004; Xu et al., 2010; Loperte et al., 2016)

2. The Medau Zirimilis Dam

The Medau Zirimilis Dam, located in the Casteddu River in southern Sardinia (Fig. 1a), is an embankment dam constructed for irrigation and water supply. The dam is southwest of Sardinia, at the transition area from the post-Hercynian materials and the metamorphic Hercynian belts (external areas of the Hercynian orogen). The reservoir is atop metasandstones and metapelites from the Middle-Upper Ordovician (Monte Argentu Fm; Funeda et al., 2009 Fig. 1b). The embankment abuts against these metamorphic rocks that present a mainly southward dip (in the upstream direction). The regional materials are composed of metamorphic units (mainly metasandstones and metapelites) and locally igneous rocks. The only unit with high clay content is the fluvial flood plain that does not show significant development. The limited availability of impermeable materials led to the construction of a massive structure without a waterproof core. The waterproof barrier is composed of an asphalt face slab that is the only impervious element. The stability and correct functionality of the dam is therefore strongly dependent on the waterproof structure that covers the upstream dam slope. The dam was constructed using materials from the pediment and terrace levels that were compacted to reach internal friction angles between 37 and 40°. The dam was completed in 1991 with a capacity of 19 Hm³, a longitude of 480 m and a maximum height of 151 m asl, reaching 44 m from the lower part of the reservoir. The waterproof barrier is a 46-cm-thick asphalt conglomerate that includes a permeable internal level for drainage purposes.

Since its construction, loss of water through the dam or its abutments has been continuous and has been detected in the boreholes downstream from the dam (Frongia, 2013). As a consequence, detailed monitoring of the piezometric level surrounding the dam has been conducted and its freeboard has increased. These conditions have motivated the structural analysis of the dam considering the stability of the slab face. During the last several years, open cracks and relative movement of the waterproof barrier, consisting of asphalt shingles, have been identified. The origin of such problems can initially be attributed to construction problems, incorrect materials or structural damage. The impervious slab was repaired and newly

reconstructed, but some years later, damage re-appeared. Because the critical element of the dam is a single and relatively thin asphalt barrier, an analysis of the barrier was performed in detail in this study. GPR has been used in dams and embankments for the identification of cavities, erosion of waterproof clay layers and internal leakage (e.g., Seje et al., 1995; Xu et al., 2010; Hui et al., 2011; Loperte al., 2011; Chlaib et al., 2014; Antoine et al., 2015).

GPR represents an interesting approach for the characterization of the impervious slab and the detection of deformation affecting the shallowest constructed units. To evaluate these features in the Medau Zirimilis Dam, a GPR campaign was conducted along its upstream face, the dam crest, the berms at the downstream slope and its lateral sectors. The objectives of the survey were to identify the presence of deformational structures involving construction materials and denoting a post-construction modification, as well as to identify the origin of the sliding of the asphalt slabs down the upstream dam side. Moreover, the objective of the survey was also to evaluate if there was a correlation between the seepage and the identified problems in the asphalt barrier of the dam.

A surficial analysis of the upstream slope shows cracks that can be ascribed to three main groups (Fig. 2a): i) subvertical cracks perpendicular to the upstream slope (normal cracks) related to the limits between asphalt tiles; in general, these have linear traces, or eventually irregular trends between shingles, with differential relative movement (shear cracks: Fig. 2a), ii) subhorizontal cracks, having interruptions or small steps at the intersection between shingles, and defining small bulges or depressions; and iii) transverse cracks, showing a vertical component, that are less representative, usually affecting the asphalt layers and their limits. Deformation of the slab surface can also be expressed without rupture, by means of slope changes along the surface, topographical internal depressions between transverse and irregular cracks, and non-linear trends between different asphalt laminae. Crack distribution highlights the construction limits and indicates apparent differential movement between panels, as shown by shear and transverse cracks pre- and post-dating the reparation of the upstream dam face (see Fig. 2b for a comparative analysis between 2004 and 2013).

2. GPR survey design, equipment and methodology.

GPR was conducted along three accessible sectors (Fig. 3): the crest of the dam, its upstream slope covered by asphalt shingles and its downstream slope at three different berms. The survey was completed with profiles along different near sectors including lateral dam zones and over the roads to the west and southwest of the dam. In the constructive sectors and following the expected technique of dam construction, GPR profiles should permit one to identify homogeneous, subhorizontal disposition or shallow dipping reflectors in the subsoil. In this sense, the survey was defined to identify non-horizontal or sharp lateral changes of reflectors underground. Because of the topography of the survey zone, zones 1 and 3 were surveyed along horizontal surfaces with a vertical propagation of GPR waves into the dam structure (Figs. 3 and 4). In the case of the upstream face, the survey was conducted along constant-elevation profiles (Fig. 4c) but the GPR wave propagation is normal to the survey surface, and the record shows an image of the dam structure at an angle with the vertical (Figs. 3 and 4c). Similar approaches have been previously employed in structures of this type (e.g., Di Prinzio et al., 2010). In this manner, topographical correction of the profiles was not necessary, and the objectives were focused on the identification of structural changes different from that expected given the dam's construction characteristics.

Because of the surficial characteristics of the surveyed zones and the objectives of the survey, three different groups of GPR antennas were used as follows: (i) 100-, 250-, and 500-MHz shielded antennas from RAMAC and a CUI-2 central unit along zone 1, (ii) 250 MHz in zone 2, (iii) 100 MHz in zone 3, and (iv) 100 MHz surrounding the dam and along the adjacent roads and lateral dams. Survey objectives were defined to evaluate non-horizontal reflectors or progressive changes that could denote post-constructive modifications or irregular trends that could suggest a subsidence process during or following the different construction phases. The surveyed zones were defined according to their accessibility and potential to evaluate the structure and dam characteristics. Zone 1 was used as a survey pilot zone (Fig. 4a and b) to evaluate the depth penetration of the GPR waves and the configuration. The homogeneous distribution of reflectors at the 100-MHz radargrams suggested focusing the analysis in the 250-MHz frequency for subsequent survey in the upstream sector where survey conditions were more difficult for low-frequency antennas. In the case of the downstream sector and the lateral

profiles (Fig. 4c and d), a survey was performed using the 100-MHz antenna to identify accommodation features related to syn- and post-construction modifications.

Processing consisted in the filtering of range frequencies, gain (linear and exponential, in some cases reaching wave saturation to maximize reflector change identification), running average for smoothing GPR-profiles, and subtracted mean trace to increase the identification of non-horizontal changes and reflectors. The complete survey consisted of more than 8.8 km of linear profiles (Fig. 4a). According to changes found in the subsoil in Zone 1, the survey configuration for the detailed and systematic survey in this sector showed penetrations of 2 m for 500 MHz and 4 m for 250 MHz. In the case of the downstream sector and the road surrounding the dam, the 100 MHz antenna reached a depth of 10 m. In all cases, a higher penetration was obtained using a 1024 sampling routine, resulting in an increase in the number of samples and depth penetration; the resolution did not diminish due to the survey configuration change (see Table 1 for configuration characteristics).

4. GPR results

Data obtained in zone 1 (the upper part of Fig. 5a and b: 500 MHz), over the crest of the dam, show irregular reflector trends, with depth variations, tilting and changes in the thickness of the uppermost, more reflective unit. This result differs from the expected structure having homogeneous layers. In some cases, changes in the thickness of the upper units exceeded 1 m (Fig. 5a and b), or tilted reflectors or non-horizontal geometries were identified below this depth. The general trends of these changes along the crest are (i) a progressive increase in thickness of the upper unit in the western abutment (Fig. 5a), showing irregularities at approximately 2 m depth, (ii) a sudden decrease in thickness of the shallowest unit at 275 m (Fig. 5b: 250 MHz), defining a relative high, and again a concave-upwards geometry between this position and 450 m. At approximately 2 m in depth, a subhorizontal reflector, parallel to the surface, was found, indicating that the described structural changes only affect the upper part of the structure. This supports the identification of surficial structural changes that do not respond to propagation from deeper levels of the dam.

Along the upstream slope (zone 2; lower part of Fig. 5, a, b and Fig. 5 c: 250 MHz) different profiles over the asphalt shingles were conducted to identify its structure and the

underground dam characteristics. The construction of the dam was completed in layers between 0.5 and 0.8 m in thickness, indicating that such intervals should be dependent on the constructive characteristics and reparations of the face slab. However, the non-horizontal reflectors below the asphalt layers indicate a deeper involved thickness. These geometrical changes involve, for certain sectors, a thickness between 2 to 3 m (Fig. 5c; 250 MHz), which is above the expected thickness for the asphalt slab. The thickness or depth of non-horizontal reflectors is higher in the upper part of the dam face than in its lower part. Therefore, similar structural changes can be identified along the whole dam side but at different depths. In addition, some isolated hyperbolic anomalies separating the GPR domains (defined by different penetration, definition of reflectors, banded distribution or reflectivity) were identified. Such anomalies were, in general, systematic and can be correlated between different profiles at the same positions. Apart from these structural changes, thickness changes of the non-horizontal sectors define the domains separated by these hyperbolic anomalies, while in other cases, structural changes, e.g., plane-concave geometries, extend over the limits between the domains.

The survey along the downstream face did not show significant changes (Fig. 6; 100 MHz). In general, homogeneous or progressive thickness changes in the reflective upper unit or horizontal and progressive tilted reflectors were identified. A similar thickness, ranging from 6 to 9 m, was interpreted along the upper and intermediate profiles, with a lower penetration occurring when approaching the natural materials below the dam. At the abutments, the upper constructive levels show a more homogeneous pattern and do not define geometries liable to be interpreted in terms of sudden changes in thickness or tilted reflectors.

5. Infrared thermographic analysis

In parallel to the analysis of the GPR survey, infrared thermography was conducted to evaluate the internal structure of the upper layers of the upstream side of the dam. Photographs were taken using an NEC TH9260 camera with a resolution of 0.06°C. This analysis can be performed during the early morning or during the last hours of diurnal insolation to measure the temperature of different materials related to the different thermal behavior of surficial and near-surface materials. The performed analysis was conducted during the last hours of the day along

the upstream side of the dam (Fig. 7) to identify thermal changes in the asphalt layers or underlying units. Obtained results permitted us to identify two groups of linear thermal anomalies, one parallel to the main slope of the dam surface and a second that is perpendicular (horizontal). This distribution is interrupted at certain sectors where the parallelism disappears and irregular trends can be identified. These trends correlate in general with the surficial limits identified during the inspection and with the hyperbolic anomalies with a direct correlation between profiles identified using the GPR.

6. Discussion

GPR results permitted us to identify, in a general, i) a sector below the dam crest with horizontal or progressively changing reflectors in most surficial units (at least in the first 2 m); ii) geometrical changes on the upstream side that progress below the expected depth for the waterproof structure, involving both horizontal (thickness and anomalies individualizing different sectors) and vertical (higher involved thickness in the upper part with respect to that of the lower part) distribution; and iii) homogeneous trends without significant changes along the downstream side and the lateral sectors of the dam.

To evaluate the correlation among the identified changes, anomalies and their distribution, an integrated analysis of the different obtained profiles was conducted. The objective of this analysis was to evaluate the position of the lower limit for irregular trends, tilted reflectors or interruption of layers. The analysis was performed by picking up the position of the lower limit of the non-horizontal areas from the different profiles, especially the 250-MHz profiles, that were the most systematically performed. A model of the correlation of the identified limits along the different profiles from survey zones 1 and 3 was completed to evaluate the degree of correlation between the profiles and their potential correlation with the identified cracks and problems affecting the asphalt layers. On the one hand, it seems that the systematic group of the hyperbolic anomalies identified in the radargrams with a direct correlation between profiles can be ascribed to the construction limits of the impervious slabs (Fig. 8) that were also identified during the thermographic analysis (Fig. 7). The comparison between the surficial movements and cracks to the underground structure shows that the sectors showing the strongest structural changes in the GPR profiles (Fig. 9) correlate with the sectors where higher

surficial movements were detected. The thickness distribution of the involved materials and non-horizontal reflectors coincide with a stronger deformation of asphalt laminae. This correlation substantiates that the surficial movements involve a greater thickness than the asphalt layers and include materials of the dam structure itself. The same methodology of correlation between profiles was also applied for the upper part of the dam (crest), although in this sector, there is no evidence of cracks affecting the survey zone. However, this analysis can permit the direct comparison of the underground structure along the crest and the upstream face (Fig. 9).

The described geophysical changes have been identified in a damaged face slab where open cracks with vertical (following the expected construction limits), horizontal or tangential orientation define downslope irregular movements of the asphalt laminae. Moreover, in some cases, the displacements are not homogeneous and present an apparent decrease from top to bottom along the upstream slope.

In the case of the dam crest, the thickness of the series with non-horizontal geometries increases at its southern boundary (near the upstream crest border). In the upstream face, sectors of greater thickness changes were identified at the upper part of the dam slope, with an irregular distribution; these results imply that a correlation of thickness changes can be established between the upstream and downstream dam shoulders. The presence of isolated hyperbolic anomalies, interpreted as construction limits, permits their correlation by thickness changes, providing an anisotropic pattern of the near-surface construction units separated by sub-vertical contacts. These changes can be correlated longitudinally (Fig. 9), with (i) an increase in thickness in the western sector that was identified both at the crest and at the southern side; (ii) a lower involved thickness in the central zone of the dam, including its southern side; and (iii) an increase towards the eastern sector that again is observed in both shoulders.

The limits of thickness changes along the southern sector of the dam show a general correlation with the open cracks and relative movements between asphalt laminae. The highest density of cracks indicates the strongest relative movement of asphalt laminae. Sectors with a smaller thickness of the non-horizontal unit identified in the GPR model usually have less

development of cracks, or at least, less relative movement. However, in many cases, the anisotropy related to the limits between the laminae and their relative movement does not allow establishment of a clear correlation between the two variables. In these cases, the thickness changes overcome the limits of the individual laminae and can produce their internal deformation (this was identified in the description of the different cracks, the photographs from the present day and the thermographic images) implying that the origin of the movement is below the asphalt layers and cuts through the construction limits.

The safety of the studied dam, without an impermeable core, lies on the impervious slab that covers its southern upstream slope. The identification of structural deformation at the shallowest levels indicates the instability of such units during, at least, the last phases of construction. Although the relationship between these changes and seepage at present is not straightforward, the correlation of the involved changes in thickness along the crest and the upper part of the upstream sector, and the identification of open cracks allowing down-dip movement of the asphalt layers, defines incipient deformation of the waterproof barrier. Moreover, the described deformation affects the impervious barrier and the underlying units, but there are no evident correlations with the known seepage in the area.

The geometrical changes identified in the GPR profiles and compared to the surficial data differ from the expected horizontal geometry and can be related to deformation affecting such levels that, at least within the reached depth, only involve the face slab and not the main dam body. In this sense, the geometrical changes and their distribution depict geometries more compatible with landslides that involve both the waterproof asphalt layers and the underlying materials along the southern sector and the crest of the dam. These results imply that the problem of the stability of the slopes and crest cannot be solved by only repairing the asphalt slab. Evaluation of these features is needed to prevent dam failure. An increase in the reservoir water level will saturate these features, affecting the stability of the southern side of the dam, and triggering shallow landslides.

Structural changes without evidence of vertical movement along the dam crest does not allow a straightforward interpretation, because such deformation does not apparently affect the survey surface. These features can be related to deformation processes in underground layers

without progression after crest completion. Unfortunately, there is not a record of this type of event during dam construction. Another possible interpretation is that deformation progresses independently in the lower levels below the rigid concrete structures along the crest. This correlation and the present-day movements identified along the upstream slope, support, with independence of the interaction between both dam slopes, the existence of anisotropies that will produce non-homogeneous behavior of the dam and probably the development of preferential flow paths and landslides. The origin of the process of subsidence during dam construction is unknown, but they can tentatively be related to weathering of units between the main dam structure and the cover due to differential behavior of the involved materials. Problems related to the propagation of desiccation cracks before the installation of the impermeable layers have been documented in embankment dams (e.g., Konrad and Ayad, 1997; Style et al., 2010; Jones et al., 2014), generating flow paths through these upper materials (Cooling and Marsland, 1954) or sliding surfaces along the shallower units. This feature, although only involving the upper surficial units, is relevant, because it is directly related to the impervious asphalt slab.

Surveillance, monitoring, evaluation and integrity characterization of the waterproof surficial barrier are necessary to guarantee the safety of the Medau Zirimilis Dam because most of the surveyed zones along the upstream slope are below the design level. This defines a complex situation due to the instability of the upstream slope and the upper part of the dam. A scenario of generalized seepage through the described limits and the triggering of landslides on the asphalt slab would produce circulation of water through the dam that, because of the pressure changes on both sides and existing anisotropies, could lead to erosion, piping and subsequent collapse of the structure. These features, as described in the introduction, are the most common conditions of embankment dam failures that can progress in a fast manner with significant consequences downstream.

The increase in embankment structures and the use of surficial hydrogeological barriers vs. the classical solution of impervious cores has increased recently because of construction in areas without suitable materials for more traditional dam construction designs (e.g., USDI; 2012). The usual handicap for penetration of GPR waves is avoided in this new type of structure, due to the absence of a clay core. This enhances GPR availability for the evaluation both of quality emplacement control or characterization of underground materials. Nevertheless,

even if GPR is sensitive to water content, the obtained results do not permit one to identify seepage areas in the studied structure, although an indirect evaluation considering the affected and non-affected areas from the dam can be established. This dynamic suggests that the used method can permit one to discard seepage as affecting, at this moment, the surveyed areas but highlights the presence of unstable sectors in the surficial barrier that require monitoring.

7. Conclusions.

The safety and erosion protection of embankment dams without impermeable cores lie in the impervious face slab. The use of an asphalt slab, that can initially be a good solution, has some drawbacks because of its near-surface position, changes in properties with respect to underground materials and interaction with solar radiation. These factors can contribute to undermining its continuity and impermeable behavior. In the case of the Medau Zirimilis Dam, seepage and water losses have led to an increase in the freeboard and a diminished reservoir capacity to prevent its failure. Successive reparations have been needed to repair open cracks and correct relative movements between the asphalt laminae in its upstream face. GPR evaluation of accessible sectors of the dam has permitted the determination that in sectors that are affected by cracks and relative movements between asphalt layers, the involved thickness supersedes the asphalt layers. The distribution of these affected volumes is interpreted in terms of surficial landslides that affect both the crest and upstream slope, indicating incipient instability of the slab. The distribution of these landslides in the proximities of the maximum allowed water level can represent an imminent hazard if these deformations are not completely repaired. This type of evaluation, integrating traditional data and thermography with GPR, can permit the interpretation of the actual origin of the problems. This interpretation allows one to focus on the needed reparations to avoid future problems, which due to the intrinsic construction characteristics, can affect dam stability.

Acknowledgements.

This work has been supported by University of Cagliari and Geotransfer Research Group from Universidad de Zaragoza. Authors want to acknowledge the suggestions developed by Dr. Wasowski as editor and two anonymous reviewers that have permitted to improve the preliminary submission version of this work.

Cited References.

AalGamal, Z.A., Ahmed, M.I., Neil, L.A., Estella, A.A., 2004. Geophysical investigation of seepage from an Earth Fill Dam, Washington County, MO. (www.dot.state.fl.us).

Antoine R, Fauchard C, Fargier Y, Durand E (2015) Detection of leakage areas in an Earth Embankment from GPR measurements and permeability logging. *International Journal of Geophysics*, volume 2015, Article ID 610172.

Barrile V, Paccinotti R (2005) Application of radar technology to reinforced concrete structures: a case study. *NDT&E Int.* 38, 596–604.

Bolève, A., Revil, A., Janod, F., Mattiuzzo, J.L., Fry, J., 2009. Preferential fluid flow pathways in embankment dams imaged by self-potential tomography. *Near Surf. Geophys.* 7 (5), 447–462.

Brosten TR, Llopis JL, Kelley JR, (2005) Using geophysics to assess the condition of small embankment dams. US Army Corps of Engineers. ERDC/GSL TR-05-17. 28p.

Bungey JH, (2004) Sub-surface radar testing of concrete: a review. *Constr. Build. Mater.* 18, 1–8.

Chang CW, Lin CH, Lien HS (2009) Measurement radius of reinforcing steel bar in concrete using digital image GPR. *Constr. Build. Mater.* 23, 1057–1063.

Chlaib H, Mahdi H, Al-Shukri H, Su MM, Catakly A, Abd N (2014) Using ground penetrating radar in levee assesment to detect small scale animal burrows. *Journal of Applied Geophysics*, 103: 121-131.

Cooling LF, Marsland A (1954) Soil mechanics studies of failures in the sea defence banks of Essex and Kent. Proc. ICE. — North Sea Floods 31 January/1 February 1953, pp. 58–73.

Di Prinzio M, Bitelli M, Castellarin A, Pisa PR (2010) Application of GPR to the monitoring of river embankments. *Journal of Applied Geophysics*, 71: 53-61.

Evans R, Frost M, Stonecliffe-Jones M, Dixon N (2006) Ground-penetrating radar investigations for urban roads. *Proc. Inst. Civ. Eng. Munic. Eng.* 159 (2), 105–111.

Forde MC, McCann DM, Clark MR, Broughton KJ, Fenning PJ, Brown A (1999) Radar measurement of bridge scour. *NDR&E International*, 32: 481-492

Frongia, P. (2013). “Studio delle problematiche delle infiltrazioni e perdite della diga di Medau Zirimilis (Sardegna SW)” PHd Thesis. Università degli Studi di Cagliari. 247 p. <http://veprints.unica.it/882/>

Funeda, A., Carmignani, L., Pasci, S., Patta, E.D., Uras, V., Conti, P., Sale, V., (2009) “Note illustrative della Carta Geologica d’Italia alla scala 1:50.000; foglio 556 Assemini”. Istituto Superiore per la Protezione e la Ricerca Ambientales. Servizio Geologico d’Italia. 192 pages. 1 map.

Hugenschmidt J (2002) Concrete bridge inspection with a mobile GPR system. *Constr. Build. Mater.* 16, 147–154.

Hui L, Haitao M (2011) Application of Ground Penetrating Radar in Dam body detection. *Procedia Engineering*, 26: 1820-1826.

ICOLD Bulletin (2013) Internal Erosion of Existing Dams, Levees and Dikes and Their Foundation. International Commission on Large Dams, Paris.

Kocbay, A., Kilic, R., 2006. Engineering geological assessment of the Obruk dam site (Corum, Turkey). *Eng. Geol.* 87, 141–148.

Konrad R, Ayad JM (1997) Desiccation of a sensitive clay: field experimental observations. *Can. Geotech. J.* 34, 929–942.

Loperte A, Bavusi M, Cerverizzo G, Lapenna V, Soldovieri D, (2011) Ground penetrating radar in dam monitoring: the test case of Acerenza (Southern Italy). *International Journal of Geophysics*, volume 2011; article ID 654194.

Loperte, A., Soldovieri, F., Palombo, A., Santini, F., Lapenna, V., (2016) An integrated geophysical approach for water infiltration detection and characterization at Monte Contugno rock-fill dam (southern Italy). *Engineering Geology*, 211: 162-170.

Mellet J (1995) Ground penetrating radar applications in Engineering, environmental management and geology. *Journal of Applied Geophysics*, 33: 157-166.

Messerklinger S (2014) Failure of a geomembranes lined embankment dam- Case study. *Geotextiles and geomembranes*, 42: 256-266.

Middlebrooks TA, *Earth Dam Practice in the United States*, ASCE Centennial Transactions Paper 2620, 1952, pp. 697-722.

Saarenketo T, Scullion T (2000) Road evaluation with ground penetrating radar. *Journal of Applied Geophysics* 43 (2–4), 119–138.

Seje C, Sam J, Anders W (1995) Radar techniques for indicating internal erosion in embankment dams. *Journal of applied geophysics* 33 (1–3), 143–156.

Style RW, Peppin SSL, Cocks ACF (2010) Mud peeling and horizontal crack formation in drying clays. Res. Rep. 10/44Oxford Centre for Collaborative Applied Mathematics.

USDI, U.S. Department of the Interior; Bureau of Reclamation (2012). Designs standards no. 13. Embankment dams. Chapter 2: Embankment Design. Phase 4 (final). Reclamation. Managing Water in the West. 100 p. <https://www.usbr.gov/tsc/techreferences/designstandards-datacollectionguides/designstandards.html>

Xu X, Zeng Q, Li D, Wu J, Wu X, Shen J (2010) GPR detection of several common subsurface voids inside dikes and dams. *Engineering Geology*, 111: 31-42.

Zhang, L.M., Chen, Q., 2006. Analysis of seepage failure of the Gouhourockfill dam during reservoir water infiltration. *Soils Found.* 46 (5), 557–568.

Zhantayev Z, Kurmanov B, Breusov N, Dauren S, Alexandr K (2013) Ground Penetrating radar survey of dam structures of Kazakhstan on example of Aktobe and Karatomar Water Storage Basins. *Open Journal of Geology*,3, 25-27.

Figure 1. (a) Location of the Medau Zirimilis Dam and reservoir in Sardinia. (b) Geological map from the studied zone (modified from Funeda et al., 2009).

Figure 2. a) Photographs from the studied zone showing deformation and cracks along the dam slope. b) Photographs from 2004 and 2013, taken before and after the last reparation, are included where cracks can be identified.

Figure 3. Conceptual sketch of the analyzed dam. The different survey zones, the used terminology and the theoretical GPR rays are included. Note that vertical scale has been exaggerated for illustration.

Figure 4. (a) Location of the GPR profiles (see Table 1 for characteristics); b) photographs from the studied zone during the geophysical survey for survey zone 1 over the dam, and b) at survey zone 2 along the upstream slope.

Figure 5. a) GPR profiles over the crest and upstream zones (see photograph for location). In the profiles, reference to the structural changes, interruption of the expected horizontal distribution and net interruptions are marked by arrows. Coincident profiles for 250 and 500 MHz are shown. b) Detailed view of profiles included in (a) and made with 250- and 500-MHz antennas are shown. Net changes, structural variations, and thickness changes of most surficial units can be identified. Meters reference from (b) is the same as that in (a) where the profile location is marked by an arrow. c) Complete profile along the lower part of the dam where net interruptions related to the construction characteristics and changes of structure, thickness and dip of reflectors can be identified along the 250-MHz profile. The profile location is marked in (a). Note that changes are in many cases limited by net hyperbolic anomalies that present a correlation between profiles and are interpreted in terms of limits between asphalt layers.

Figure 6. GPR profiles conducted along the downstream slope at different heights along the construction berms. A photograph with the location of the profiles is also included. All the profiles were conducted using 100-MHz antennas.

Figure 7. - Thermographic photographs from different sectors of the dam.

Figure 8. Model of involved thickness of deformed units along the crest and upstream slope of the dam obtained from the integration of the different profiles (a photograph with the location of the studied sectors is also included). In the model developed over the asphalt slab, hyperbolic anomalies with a direct correlation between profiles and the surficial identified cracks are shown.

Figure 9. Oblique models showing a correlation of deformed sectors identified in the GPR profiles at the crest and upstream slope. Isolated anomalies with lateral correlation and cracks identified in the asphalt are also included. Note that the cracks are drawn using the most recent aerial photograph in the area (2013) after repairing and reconstruction.

Table 1. Summary of the characteristics and the location of the GPR profiles conducted in this study.

#profile	Cf	survey	TWT(ns);samples	Depth	Survey zone
(1)	100	485.25	1254 (1024)	60.86	(1) Dam top
(2)	100	483.26	497 (1024)	24.16	(1) Dam top
(3)	100	484.77	497 (1024)	24.16	(1) Dam top
(4)	100	484.08	497 (1024)	24.16	(1) Dam top
(5)	100	377.73	1277 (1024)	94.65	(1) Western access road
(6)	100	383.21	757 (1024)	96.3	(1) Western access road
(7)	100	363.01	757 (1024)	96.3	(1) Western access road
(8)	100	337.82	757 (1024)	96.3	(1) Western access road
(9)	100	405.79	757 (1024)	96.3	(1) Western access road
(10)	100	315.77	733 (1024)	34.99	(3) Downstream (upper
(11)	100	329.24	473 (1024)	55.45	(3) Downstream (upper
(12)	100	237.26	473 (1024)	55.45	(3) Downstream (lower
(13)	100	241.61	757 (1024)	96.3	(3) Downstream (lower
(14)	100	144.61	497 (1024)	24.16	(3) Downstream valley
(15)	100	139.68	237 (1024)	11.55	(3) Downstream valley
(16)	100	27.16	237 (1024)	11.55	(3) Downstream valley
(17)	250	484.49	449 (1024)	21.83	(1) Dam top
(18)	250	479.5	189 (1024)	9.23	(1) Dam top
(19)	500	480.66	189 (1024)	9.05	(1) Dam top
(20)	500	481.76	104 (1024)	4.97	(1) Dam top

(21)	250	111.25	189 (1024)	9.08	(2)	Upstream level 1
(22)	250	332.25	189 (1024)	9.08	(2)	Upstream level 1
(23)	250	438.66	189 (1024)	9.08	(2)	Upstream level 2
(24)	250	399.01	189 (1024)	9.08	(2)	Upstream level 3
(25)	250	384.08	189 (1024)	9.08	(2)	Upstream water level

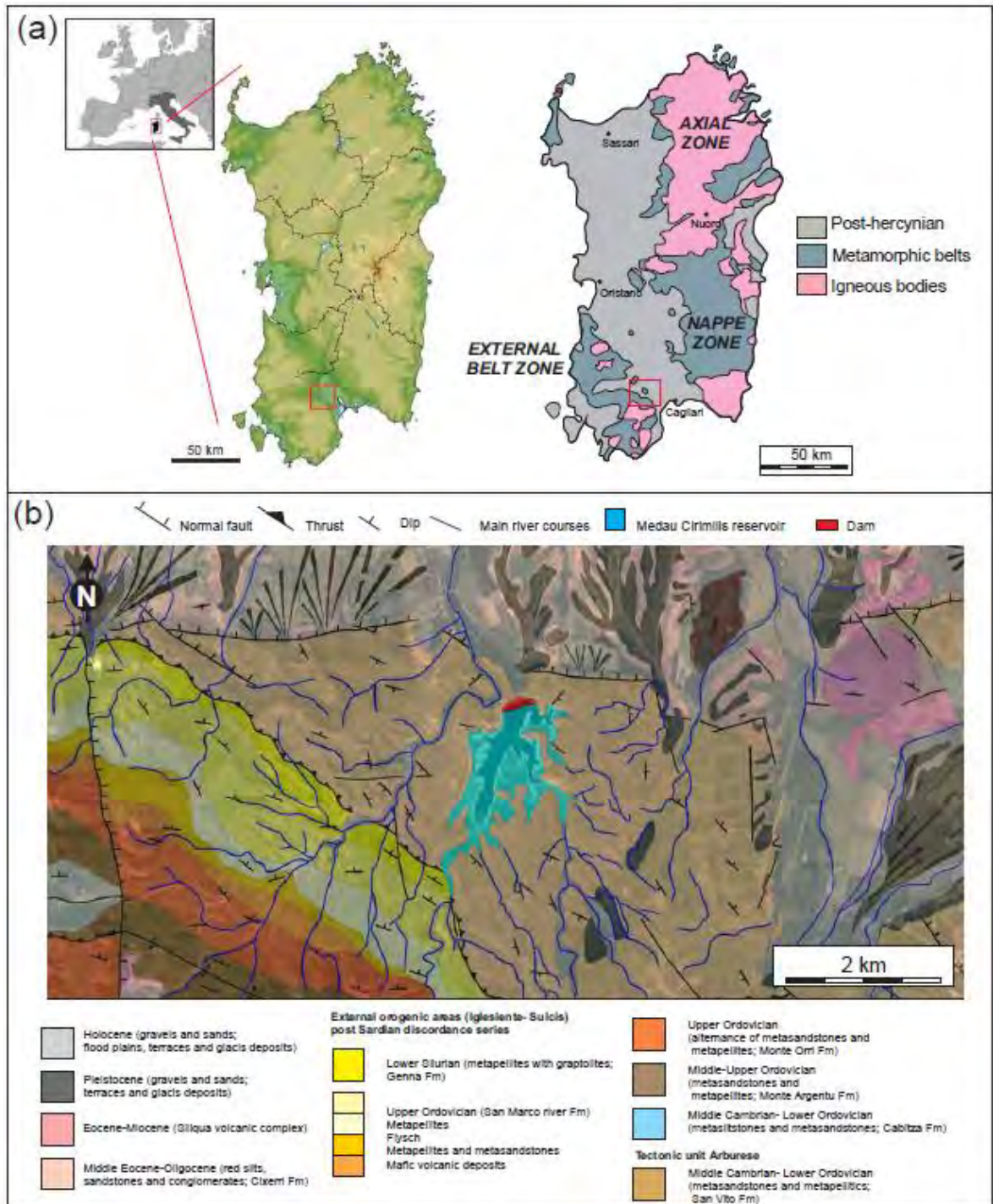


Figure 1

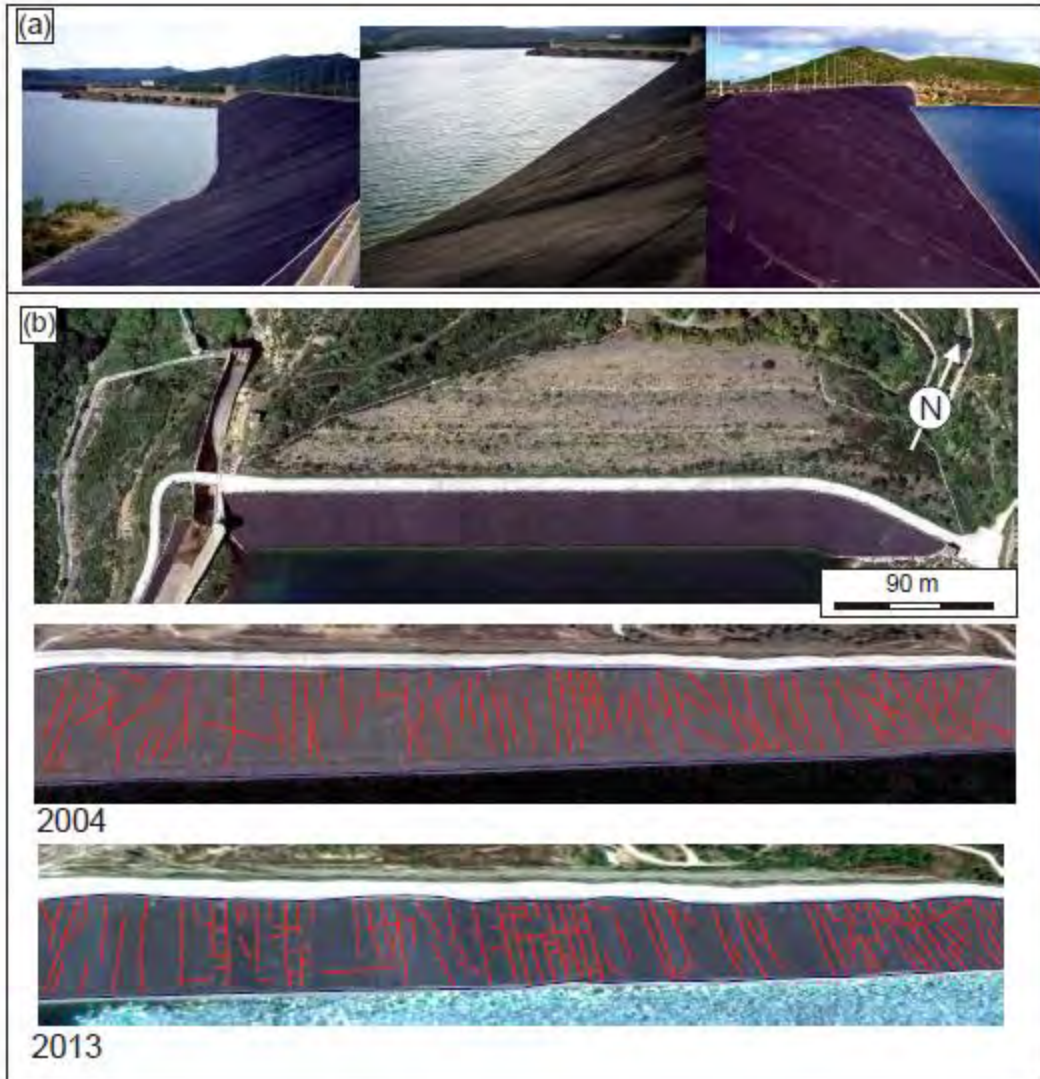


Figure 2

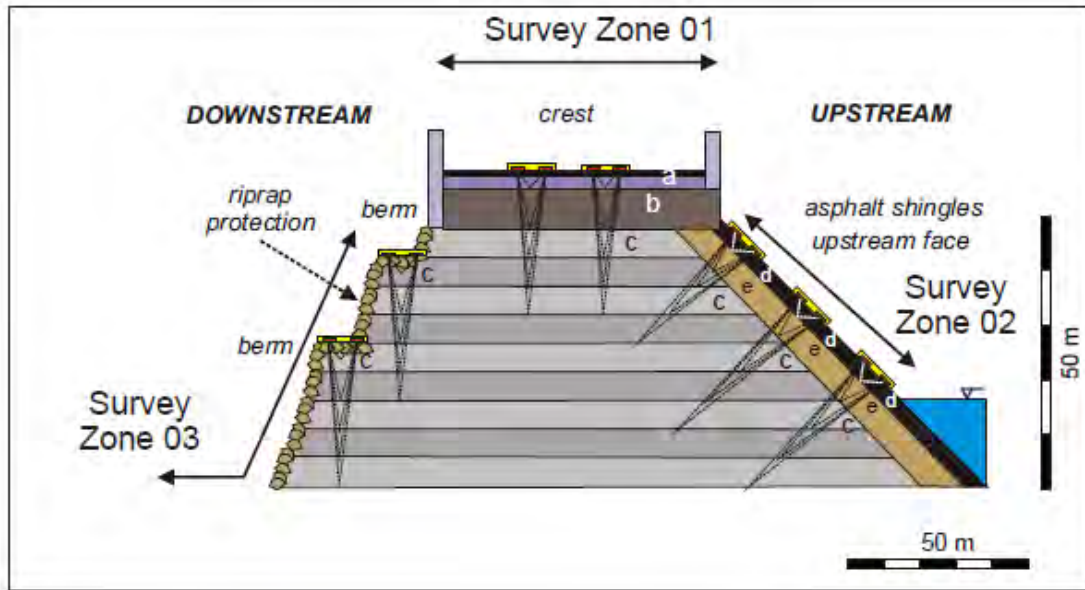


Figure 3



Figure 4

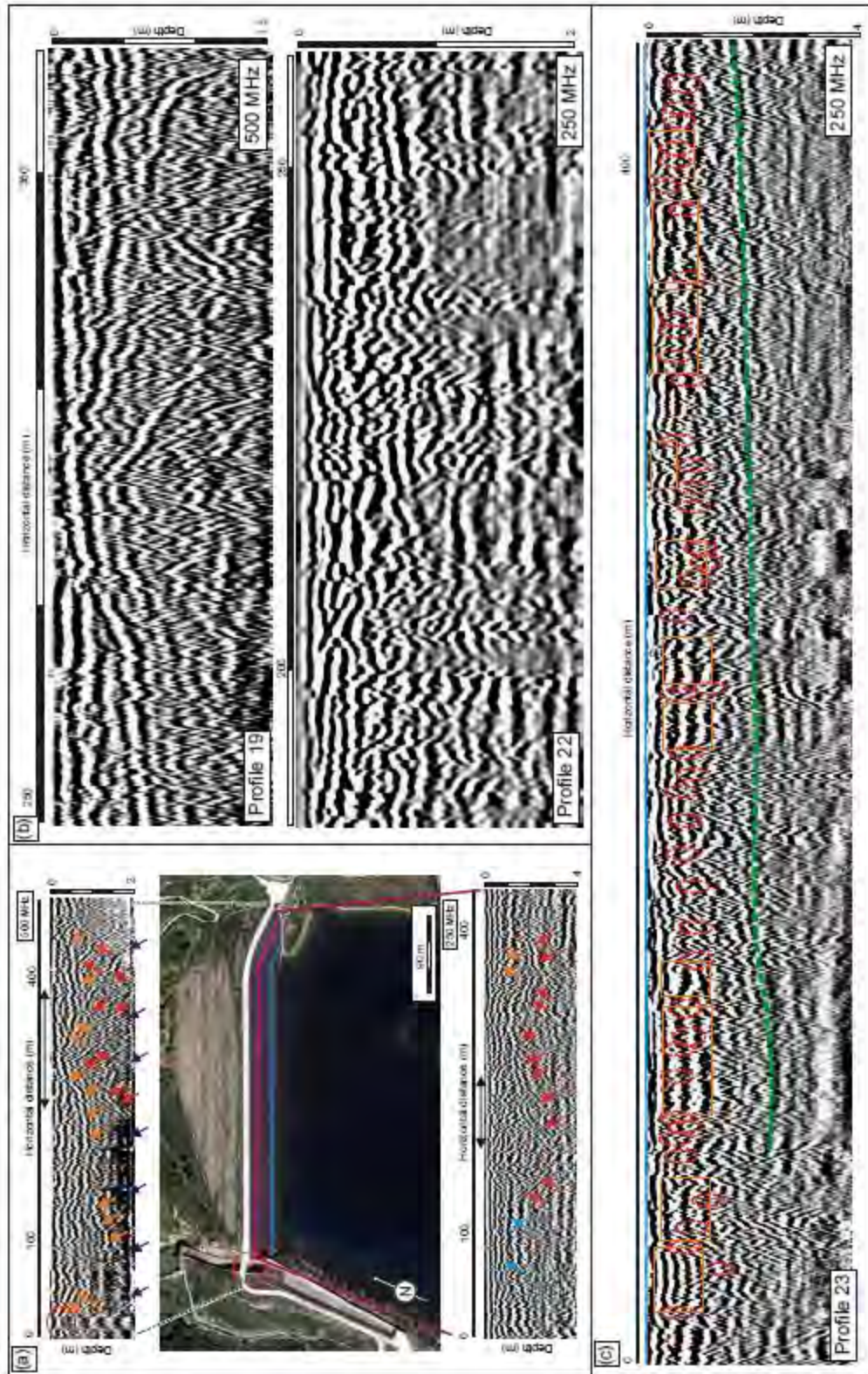


Figure 5

Figure 5.-

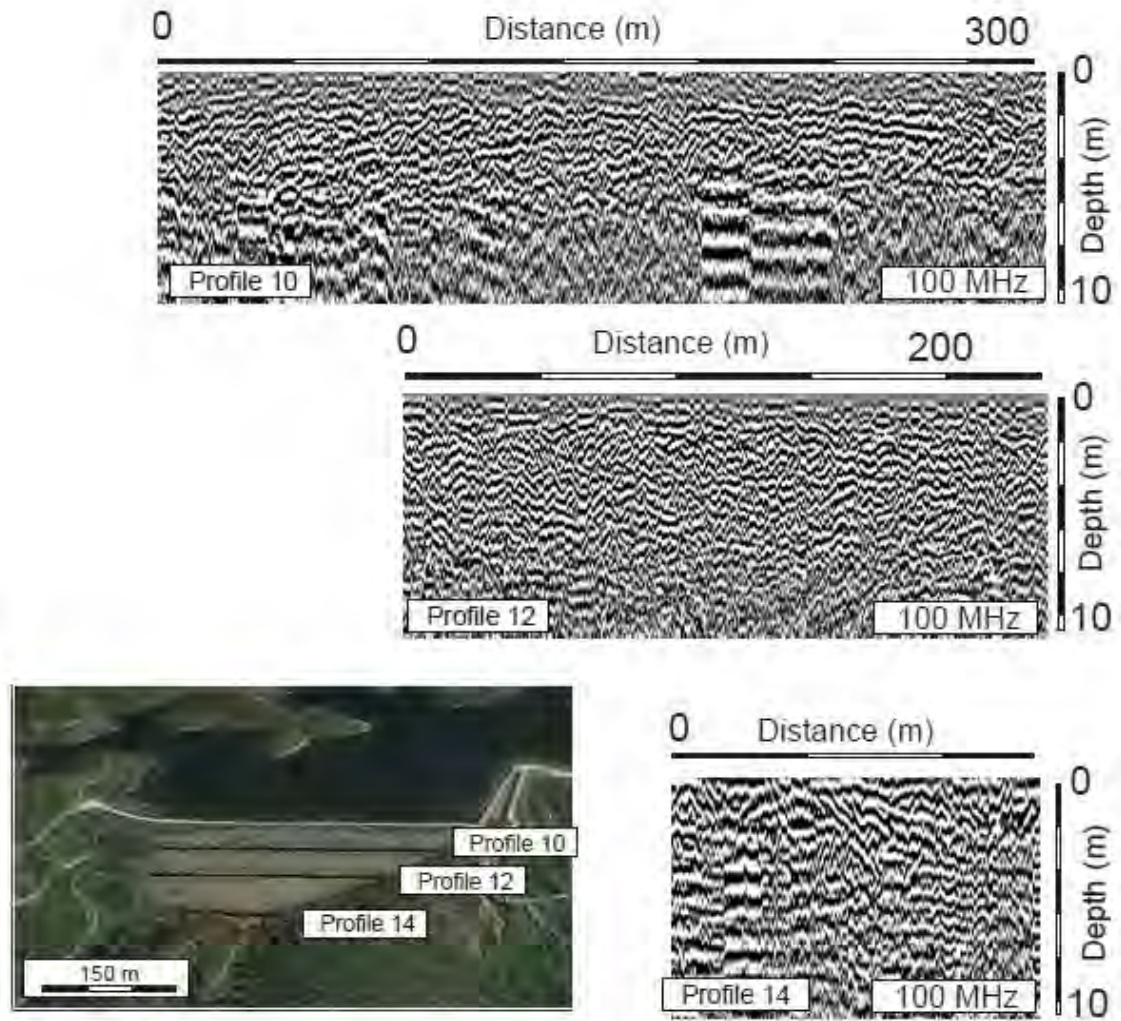


Figure 6

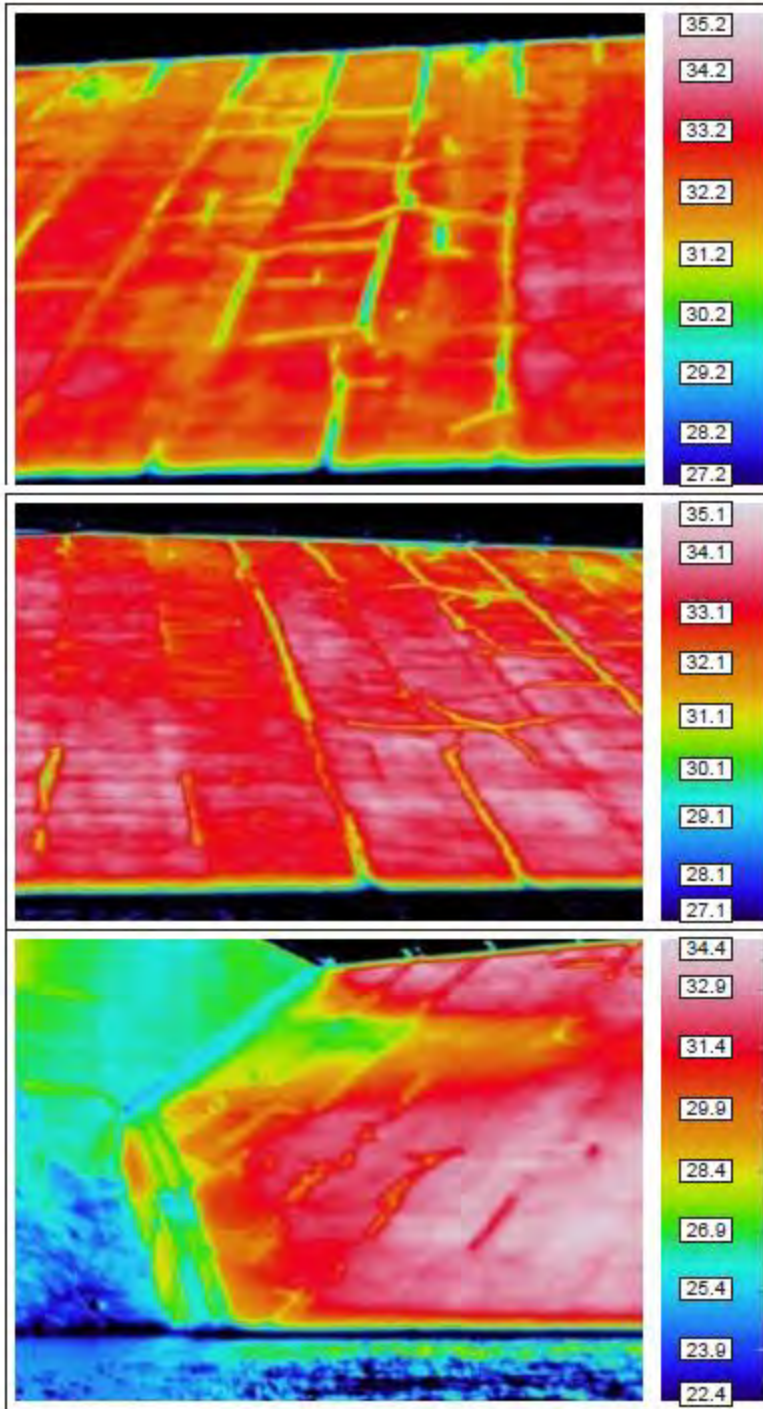


Figure 7

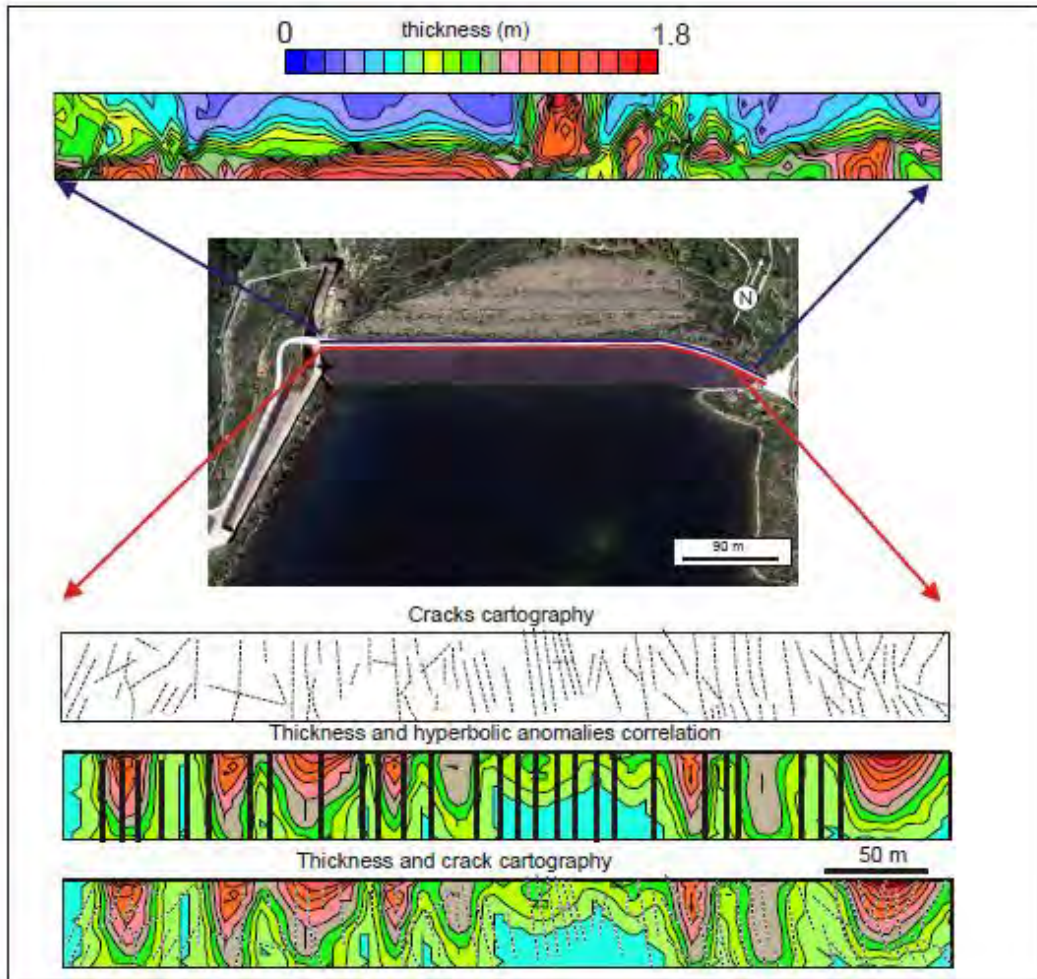


Figure 8

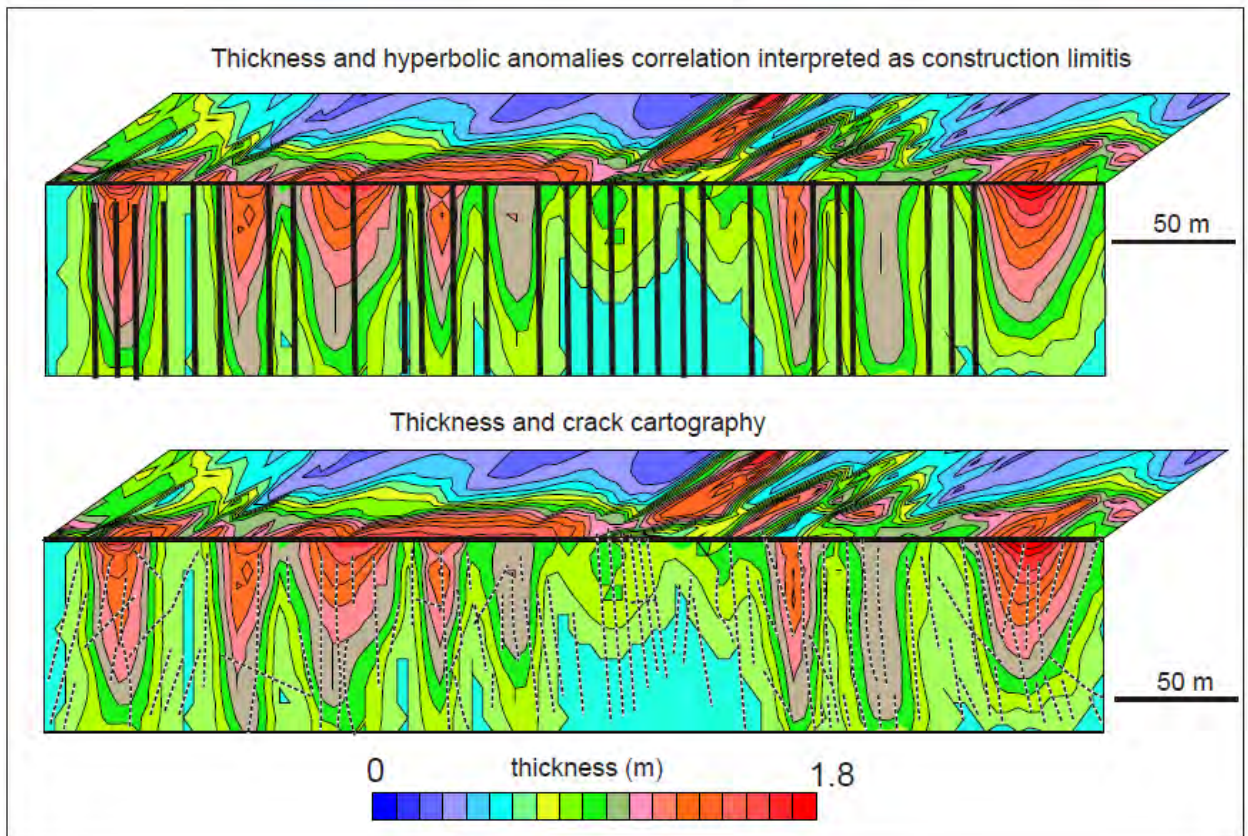


Figure 9

Highlights

- GPR analysis of the surficial structure of an embankment dam.
- Surficial slides affecting to asphalt singles at the face dam slab.
- GPR as a quality control technique or periodical monitoring survey.